

乱流における速度ゆらぎの間欠性：4.2KでのHeガスの実験

INTERMITTENCY OF VELOCITY FLUCTUATIONS IN TURBULENCE : AN EXPERIMENT AT 4.2K.

A. Naert⁽²⁾, B. Castaing^{(1)*}, B. Chabaud⁽¹⁾, F. Chillà⁽³⁾, B. Hébral⁽¹⁾, J. Peinke⁽⁴⁾

(1) CRTBT-CNRS, BP 166, 38042 Grenoble Cedex 9, France

(2) RIEC, Tohoku University, 2-1-1 Katahira Aobaku Sendai 980-77, Japan

(3) Ecole Normale Supérieure de Lyon, 46 Allée d'Italie 69 364 Lyon, France

(4) Experimental Physik II, Universitat Bayreuth, D-95440 Bayreuth, Germany

* Also at Institut Universitaire de France

Among the most important questions about turbulence, is the origin of intermittency in a flow. Another, closely related, is whether there is an ultimate, high Reynolds number regime, and if so, how it arises and how to characterize it.

The main difficulty in studying these questions is that an experiment usually gives access only to a limited range of Reynolds numbers. Physicists have to compare results from different experimental configurations, such as grid, jet and tunnel flow with the hope that the Taylor based Reynolds number R_θ is the unique and universal parameter for turbulence [1].

With cryogenic experiments using gaseous ^4He [2] it becomes possible to cover a large range of R_θ with the same geometry. Close to its critical point (2.2 bar, 5.2 K), gaseous Helium has the smallest known kinematic viscosity ($\nu = 2 \cdot 10^{-8} \text{ m}^2/\text{s}$), but can be an appreciably viscous fluid at low pressure P ($\nu P = \text{const.}$) [3]. We have built the first open flow working under such conditions, an axisymmetric jet. We have developed the corresponding anemometry techniques [4]. In the following we present briefly the experimental set-up and the anemometer. Then we discuss the velocity intermittency results at inertial scales in developed turbulence, and a new method of analysis using conditional histograms.

THE EXPERIMENTAL SET UP

The experimental system consists of a chamber (fig.1) immersed in a liquid ^4He bath which also acts as a ballast for the working gas. After laminarization, this gas enters the chamber through a contracting nozzle of section ratio 100 and diameter 2mm. The jet develops downward in the chamber, and is pumped outward to ensure the circulation. The return flow is isolated from the jet by a jacket.

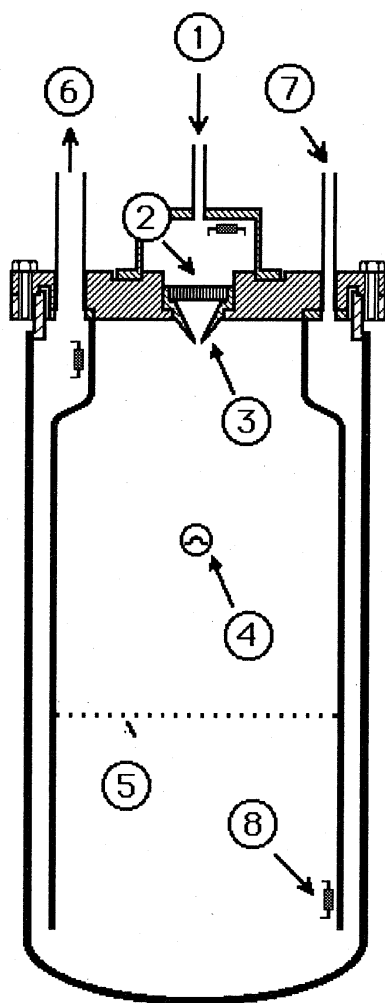


Fig. 1: Experimental set-up: (1) gas injection, (2) laminarization honeycomb, (3) nozzle, (4) detector, (5) stabilization grid, (6) pumping exit, (7) pressure measurement, (8) symbol for thermometer, (9) jacket.

An exact scale reproduction of the set-up has been made out of glass to visualize the flow with dyed water. It showed that a grid is necessary downstream to stabilize the jet. Without it, the jet randomly attaches to the walls, producing strong bursts. For more details on this point, see ref.[5].

Our anemometer is a cryogenic adaptation of the hot-wire technique using superconducting materials [4]. Its typical space resolution is about 10 μm . The wire is operated at "constant temperature" (constant resistance) through a home-made 10 MHz lock-in amplifier. The total response time to a perturbation can be less than 1 μs depending on the loop gain [4]. The voltage signal is recorded through a 12 bit HP 5183 A/D converter driven by a Macintosh Quadra 700 computer. The average signal is about 3.5 to 5.5 V, and the instrumental noise is about $10^{-7}\text{V}^2/\text{Hz}$. The calibration of the wire was made in the potential cone of the jet as described in ref. [6].

The probe is placed on the axis of the jet at a distance of 50 times the nozzle diameter (10cm), 7cm upstream from the grid. At this distance, the diameter of the jet is about 3 cm and the diameter of the jacket is 13 cm. The mean velocity U , the turbulent ratio (25%) and the dissipation rate are in agreement with what is commonly observed [7].

It is traditional [1] to study intermittency by investigating the statistics of the velocity differences δv_r between two times at the same probe. This time lag τ is converted to a distance $r=U\tau$ using the Taylor frozen turbulence hypothesis.

For each Reynolds number, a sample of 10^7 data points is recorded. A typical sampling frequency at $R_\theta=700$ is 60kHz and the whole recording time is less than 10 minutes.

EXPERIMENTAL RESULTS

We investigate the shape of the probability density function (hereafter PDF) of δv_r and its evolution with the scale, r , for different Reynolds numbers. We discuss it in terms of the parameter $\lambda^2(r)$.

It is well known that the shape of these PDFs depends on the scale, r . It goes from nearly Gaussian at large scales, L , to nearly exponential at small (Kolmogorov) scales η , where dissipation occurs [1]. The PDF at scale r can be written in a normalized way :

$$\frac{1}{\sigma_r} P_r \left(\frac{\delta v_r}{\sigma_r} \right) \quad (1)$$

which defines the function P_r (σ_r^2 is the variance of δv_r). We represent this PDF at scale r by a superposition of large scale PDFs [8] :

$$\frac{1}{\sigma_r} P_r\left(\frac{\delta v_r}{\sigma_r}\right) = \int_{-\infty}^{+\infty} G_r(\ln\sigma) \frac{1}{\sigma} P_L\left(\frac{\delta v}{\sigma}\right) d\ln\sigma \quad (2)$$

The physical basis of this superposition is given by the analysis of conditional histograms. In the Kolmogorov-Obukhov theory [1,10] G_r is simply Gaussian :

$$G_r(\ln\sigma) = \frac{1}{\lambda\sqrt{2\pi}} \exp\left[-\frac{\ln^2\left(\frac{\sigma}{\sigma_m}\right)}{2\lambda^2}\right] \quad (3)$$

It has been shown in previous papers [9,11] that the shape of P_r weakly depends on the actual shape of G_r . P_r is mainly determined by the variance $\langle(\ln\sigma)^2\rangle$. We then fit the histogram of the increments δv_r with the formula (2) using the simple gaussian distribution (3) as an ansatz. The value of λ^2 which gives the best fit of the histogram will be to a good approximation equal to $\langle(\ln\sigma)^2\rangle$.

We can then characterize the change of shape of the histograms with scale, simply by investigating the r dependence of λ^2 . Fig. 2 illustrates the assertion that the shape of P_r mainly depends on λ^2 . PDFs corresponding to measurements at several Reynolds numbers and various scales r , but having the same measured λ^2 have been plotted versus $\delta v_r/\sigma_r$. The difference between them is small. The function P_r corresponding to this value of λ^2 is shown by a solid line.

Within the energy cascade scheme, the measured λ^2 can be interpreted as proportional to the number of cascade steps [9]. We named this important physical quantity "cascade depth".

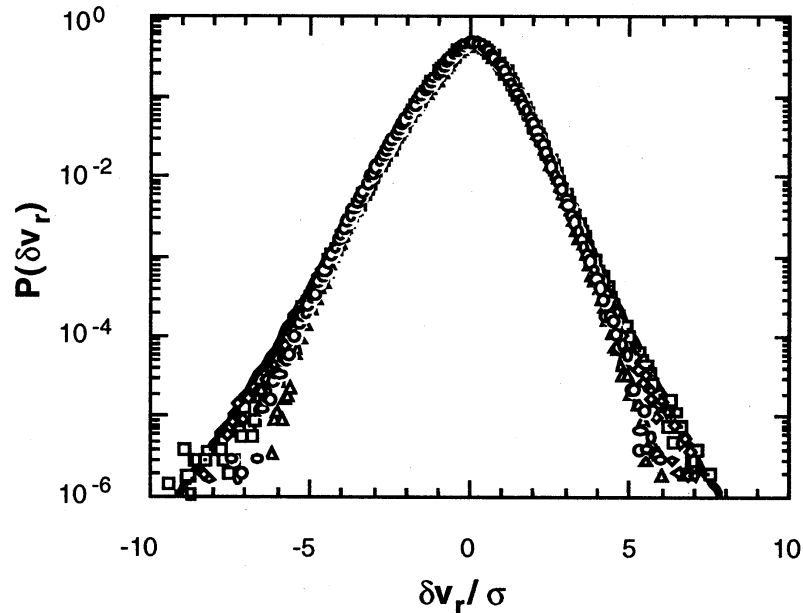


Fig. 2: Histograms of δv_r (the variance is normalized to 1) for different Reynolds numbers and different scales but the same value of λ^2 . The open symbols correspond to the following parameters (η is the dissipative Kolmogorov scale) : triangle, $R_\theta=90$, $r=20\eta$; circle, $R_\theta=161$, $r=24\eta$; diamond, $R_\theta=328$, $r=24\eta$; square, $R_\theta=598$, $r=62\eta$. The solid line represents the PDF calculated with $\lambda^2=0.09$.

There are two theoretical prediction for the behaviour of λ^2 versus r . One is the Kolmogorov-Obukhov logarithmic law $\lambda^2 \propto \ln(r/L)$, the other is a power law $\lambda^2 \propto r^{-\beta}$ predicted by the variational model [11]. It has been observed in several flows [11,12] that λ^2 might be closer to the power law than to the logarithmic law, even though we can observe in fig. 3a the existence of the latter over a narrow range at large scale. In order to firmly establish on a purely experimental basis the power law dependence, we differentiate $\ln(\lambda^2)$ versus $\ln(r)$. This is possible thanks to the quality of our determination of λ^2 by systematically minimizing a X^2 quantity [9]. We observe in fig. 3b a plateau region which is a clear affirmation of the power law dependence of λ^2 in this range.

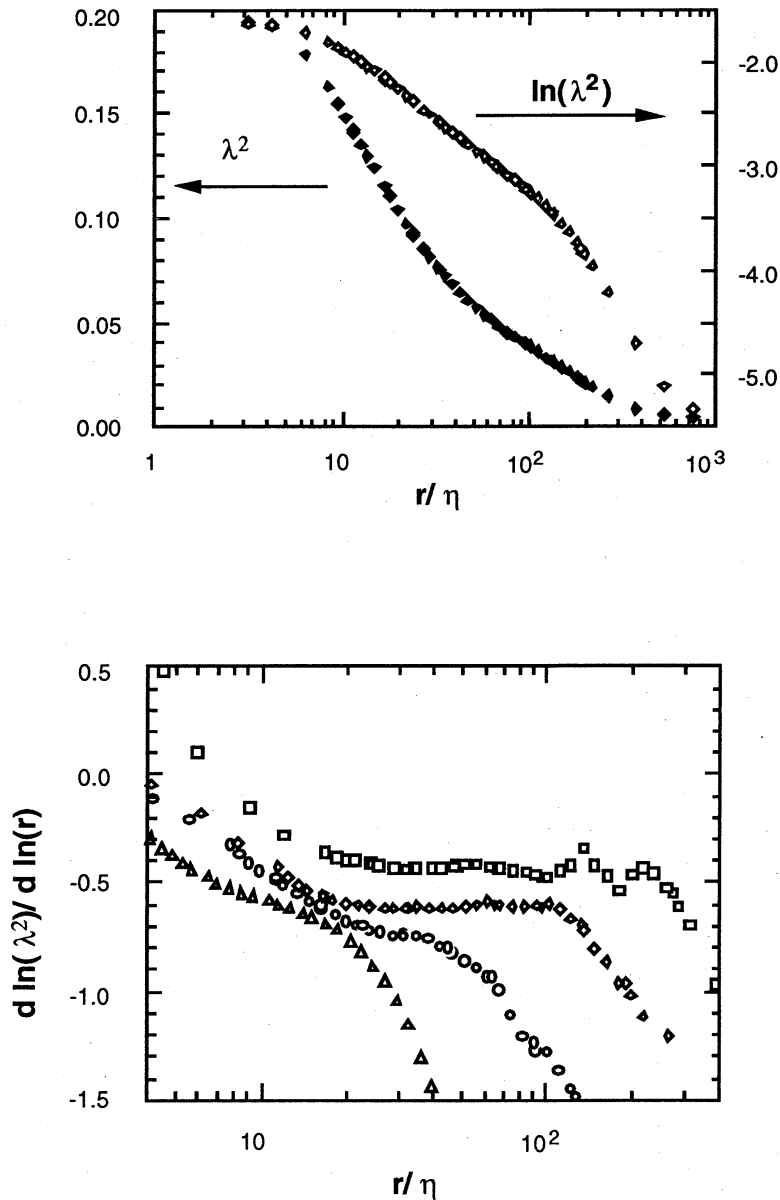


Fig. 3 (a): Dependence of λ^2 on r for $R_0=328$. The solid diamond corresponds to a logarithmic-linear plot, whereas the open diamond corresponds to a double logarithmic plot.

(b): $d \ln(\lambda^2)/d \ln(r)$ as a function of r for different R_0 values (the different symbols represent the same parameters as in fig. 2).

The exponent $-\beta$ which is the derivative $d \ln(\lambda^2)/d \ln(r)$ in the plateau region, has been measured in the whole range of accessible Reynolds

numbers and compared to previous experiments. Following the proposed scaling of β [11], we plotted $1/\beta$ versus $\ln(R_\theta)$ in fig. 4. Good agreement is found with other jet experiments. It is thus possible to characterize with only one exponent β the whole statistics of the velocity fluctuations within the scaling range.

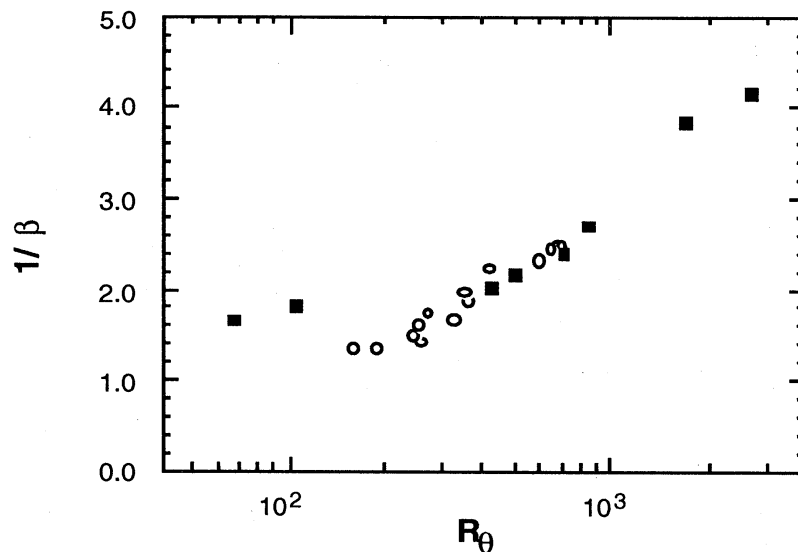


Fig. 4: Inverse of the scaling exponent β as a function of R_θ . Open circles are the results of our cryogenic jet experiment. The solid squares correspond to the same analysis for different experiments (see ref. [12]). The four middle ones correspond to air jets, the two smallest ones in R_θ to grid flow and the two highest ones to wind tunnel measurements.

Coming back to fig. 3b, we note that the plateau disappears for the lowest Reynolds number. This is a signature of the transition by which the flow goes from "hard turbulence" [13] in which the inertial range can be assimilated to the plateau region, to "soft turbulence" in which no inertial range is evident. This transition occurs at $R_\theta = 160 \pm 40$, which explains why we report no value of β below this threshold, even though we have done measurements down to $R_\theta = 90$.

Curiously enough, the grid experiments referred to in fig. 4 give values of β for R_θ below the transition. It is possible that the turbulence produced in the wake of a grid is qualitatively different from that produced by jets or wind tunnels.

Looking again at fig. 3b, we note the analogy with the isotherms of a thermodynamic liquid-gas system. The transition between soft and hard turbulence is then analogous to a critical point. This thermodynamic analogy has been developed in ref. [14].

As often, the nature of the transition gives a hint to characterize the turbulent states above and below. At low Reynolds numbers, the soft turbulence could be said to be dissipative in nature, as the scales in which energy is injected and those at which it is dissipated overlap. At large R_θ , in hard turbulence, the plateau introduces a clear inertial separation between these scales.

CONDITIONAL HISTOGRAMS

It has been found recently that a condition applied to velocity increments selects Gaussian histograms [15]. The conditional statistics are Gaussian from the inertial range down to the dissipative one. The authors used as condition $e_r(x) = \text{constant}$, the function e_r being defined as :

$$e_r(x) = \frac{15\nu}{r} \int_x^{x+r} \left(\frac{\partial v(x')}{\partial x'} \right)^2 dx' - 15\nu \left(\frac{\delta v(x)}{r} \right)^2 \quad (4)$$

The first term of the sum is the dissipation averaged over a volume of size r , in the case of locally isotropic turbulence. The second term can be seen as the dissipation at scale r . The difference e_r thus reflects the energy transfer rate at the considered scale r .

We worked out this calculation with our velocity signal, and found the following features [5] :

1) The conditional PDFs are Gaussian as we can see in fig. 5 for a few values of the condition. This is valid not only in the inertial but also in the dissipative range.

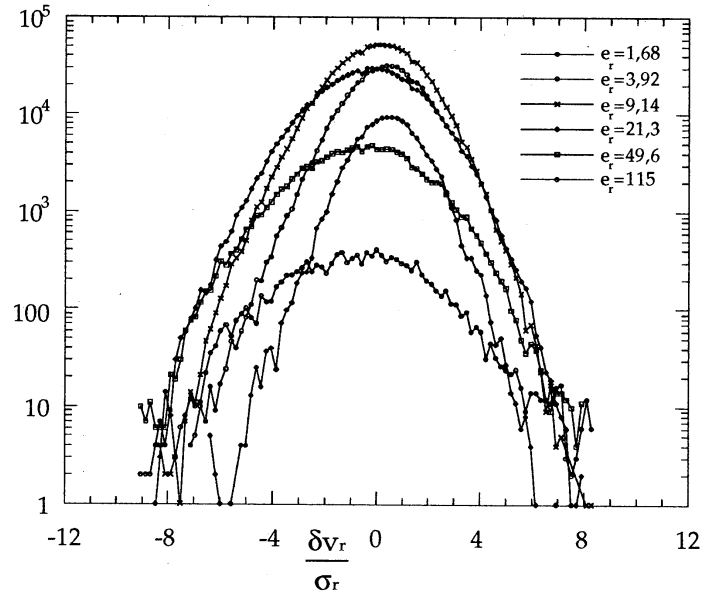


Fig. 5: Conditional histograms of the increments δv_r at scale $r=100\eta$ for a few values of the condition e_r (mW/kg). Here, $R_\theta=328$.

2) The larger the energy transfer rate, e_r , the wider the Gaussian conditional histogram : the variance of the conditional PDF is related to the condition e_r by a power law as can be seen in fig. 6 for several scales.

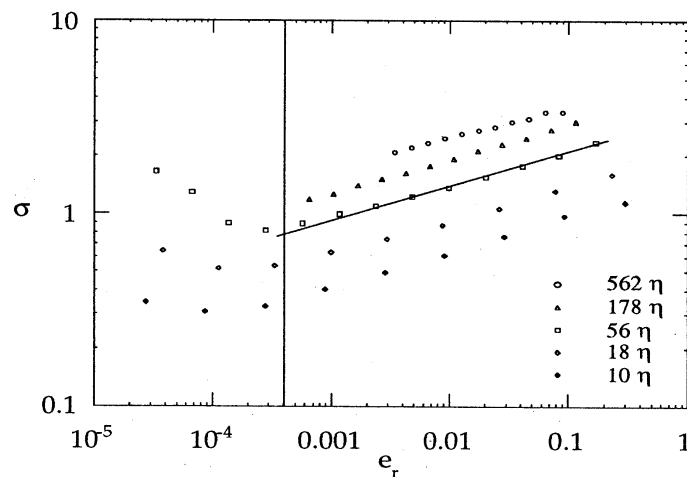


Fig. 6 : Standard deviation σ of the conditional histograms as a function of the condition e_r at several scales. The vertical line gives the limit of resolution of e_r . Here, $R_\theta=328$.

This relation gives a physical basis to the measurement method of λ^2 . Indeed, the mixture of pure Gaussian regimes supposed by equation (2) now appears natural.

3) We can easily compute the PDF of the quantity e_r by integrating the joint histogram over all possible increments δv_r . The result for various scales can be seen in fig. 7.

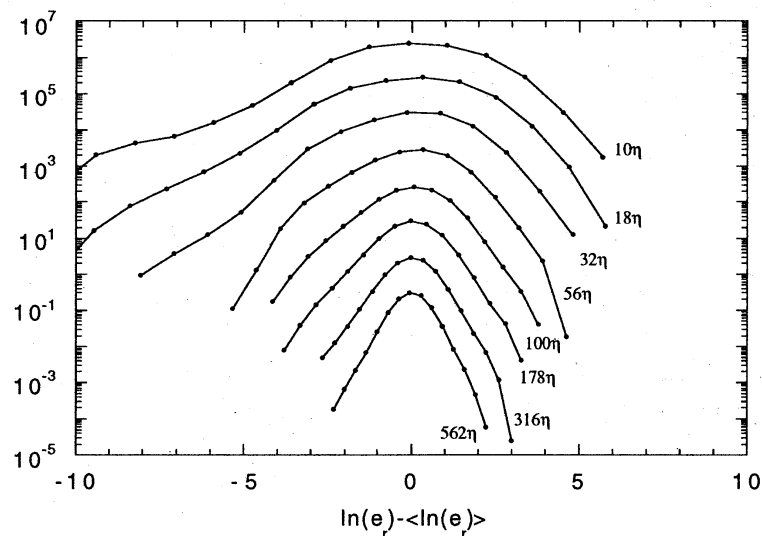


Fig. 7 : Histograms of the condition e_r at several scales. Each of these has been shifted vertically by a factor 10. $R_0=328$.

As e_r is related to σ , this gives a way to check the validity of the log-normal ansatz. But as we have already mentioned, the statistics of velocity increments are weakly sensitive to the shape of the PDF of σ . As a consequence, a very large statistical sample of velocity is necessary to make any statement on this PDF. Our sample of 10^7 points is slightly above the limit of statistical noise as evaluated in [9]. At this point we cannot determine whether the distribution of e_r (or σ) is log-normal or not.

CONCLUSION

We have built an original cryogenic experiment allowing broad variation of Reynolds number in the same geometry. Measuring the physical quantity λ^2 which characterizes the intermittency, we have shown for the first time that the inertial range appears in a turbulent flow through a well defined "second order" transition (analogous to a critical point).

The Reynolds number dependence of the exponent β shows that viscosity has some influence far beyond the dissipative (Kolmogorov) scale, up to the vicinity of the integral scale. This result is of prime importance for characterizing turbulent flows when the small scale resolution cannot be reached, for instance in large eddy simulations.

The conditional statistics of the velocity fluctuations give new insight into the structure of the cascade process. We have shown that the non-Gaussian statistics of the velocity fluctuations is due to a mixing in the flow, of "pure" (Gaussian) regimes. Behind the non-Gaussian behaviour of the velocity fluctuations, there is a hidden simple dynamics, though it is not yet understood.

REFERENCES :

- [1] A. S. Monin and A. M. Yaglom, Statistical Fluid Mechanics (The MIT Press, Cambridge, 1975)
- [2] Closed flows have already been studied in such conditions. See for instance, D. C. Threfall, J. Fluid. Mech. **67**, 17 (1975); M. Sano, X. Z. Wu, and A. Libchaber, Phys. Rev. A **40**, 6421 (1989); P. Tabeling, G. Zocchi, and J. Maurer (to be published).
- [3] R. D. McCarthy, Nat. Bur. Stand. (US) Tech. Note No. 631.
- [4] B. Castaing, B. Hébral, and B. Chabaud, Rev. Sci. Instrum. **63**, 4167 (1992).
- [5] A. Naert, Thesis, Université Joseph Fourier (Grenoble, France), 1995 (unpublished)
- [6] B. Chabaud, Thesis, Université Joseph Fourier (Grenoble, France), 1992 (unpublished)
- [7] R. A. Antonia, B. R. Satyaprakash, and A. K. M. F. Hussain, Phys. Fluids **23**, 695 (1980)

[8] The well known asymmetry of the PDF (skewness) is here entirely contained in P_L .

As in ref. [11], we use the following ansatz :

$$P_L(x) = A \exp\left[-\frac{x^2}{2}\left(1 + a_s \frac{x}{(1+x^2)^2}\right)\right]$$

where $a_s = 0.18$ and A is a normalization constant.

[9] A. Naert, L. Puech, B. Chabaud, J. Peinke, B. Castaing, B. Hébral, *J. Phys. II (France)*, **4**, 215 (1994).

[10] A. N. Kolmogorov, *J. Fluid Mech.* **13**, 82 (1962), A. M. Obukhov, *J. Fluid Mech.* **13**, 77 (1962)

[11] B. Castaing, Y. Gagne, E. Hopfinger, *Physica (Amsterdam)* **46D**, 177, (1990).

[12] B. Castaing, Y. Gagne, M. Marchand, *Physica (Amsterdam)* **68D**, 387, (1993).

[13] While the mechanisms are different in convective flows, it is worth noticing that, in this case, the transition from "soft" to "hard" turbulence has been also associated with the development of an inertial range. See F. Heslot, B. Castaing, and A. Libchaber, *Phys. Rev. A* **36**, 5870 (1987).

[14] F. Chillà, B. Chabaud, A. Naert, J. Peinke, B. Castaing, and B. Hébral, in "Proceedings of the 5th European Turbulence Conference", Sienna, Italy, 1994, Edited by R. Benzi (to be published).

[15] Y. Gagne, M. Marchand, B. Castaing, *J. Phys. II (France)*, **4**, 1-8 (1994).